Analysis of Ga As Ga Sb Ga As structures under optical excitation considering surface states as an electron reservoir

Hong-Wen Hsieh and Shun-Tung Yen

Citation: Journal of Applied Physics **105**, 103515 (2009); doi: 10.1063/1.3129616
View online: http://dx.doi.org/10.1063/1.3129616
View Table of Contents: http://scitation.aip.org/content/aip/journal/jap/105/10?ver=pdfcov
Published by the AIP Publishing

Analysis of GaAs/GaSb/GaAs structures under optical excitation considering surface states as an electron reservoir

Hong-Wen Hsieh and Shun-Tung Yen[a)]
Department of Electronics Engineering, National Chiao Tung University, 1001 Ta-Hsueh Road, Hsinchu, Taiwan 30050, Republic of China

(Received 27 February 2009; accepted 8 April 2009; published online 22 May 2009)

We present a self-consistent model for the analysis of the carrier distribution, the band profile, and the transition energy of type-II aligned GaAs/GaSb/GaAs structures under optical excitation. The model considers the surface states as an electron reservoir, associated with pinning of the conduction band Fermi level at the midgap. In our model, the optical generated holes in the GaSb quantum well causes a potential well on one side of the GaSb layer, which can efficiently accommodate the optically generated electrons. Accordingly, we derive a relation connecting the excitation power to the carrier density. Using the relation and the effective triangular potential approximation, we obtain a simple formula for the transition energy shift as a function of the excitation power, which follows the cube-root rule quite well. The calculation allows the determination of the band offset of a type-II heterointerface by comparison with data from photoluminescence measurement. The result suggests the unstrained valence band offset of GaSb/GaAs to lie between 0.5 and 0.55 eV. We also present a simplified model for analyzing the electronic and optical properties of type-II heterostructures without the need of a self-consistent calculation. © *2009 American Institute of Physics*. [DOI: 10.1063/1.3129616]

I. INTRODUCTION

The GaSb/GaAs heterostructures have received much attention because of their peculiar type-II band alignment that can cause interesting electrical and optical properties. The state-of-the-art epitaxy technology has permitted growth of high-quality GaSb quantum wells (QWs) and self-assembled quantum dots embedded in the GaAs matrix.[1–5] However, until now there still lacks a compelling unambiguous figuration for the band alignment. The difficulty in determining the band offset arises from the abnormal band profile of the highly strained GaSb/GaAs structure which may be influenced by external pumping in photoluminescence (PL) measurement. It therefore requires an appropriate model along with an ingenious experimental arrangement to explore the detail about the band profile.

There have been a few studies attempting to figure out the electronic structure of the GaSb/GaAs QW.[1–8] Ledentsov *et al.*[2] made a theoretical calculation of PL peak energy for the GaSb/GaAs structure but found a large discrepancy. Lo *et al.*[3] attributed the discrepancy to the choice of an incorrect valence band offset (VBO) and estimated the unstrained VBO for the GaSb/GaAs alignment to be about 0.4 eV from their PL measurement and theoretical calculation. Qteish and Needs[6] used self-consistent pseudopotential techniques to determine the band offset. They found a strained VBO of 1.1 eV, corresponding to a high unstrained VBO of 0.88 eV. Nakai and Yamaguchi[7] predicted an even higher VBO value from the PL transition energy for 1 monolayer (ML) GaSb/GaAs QW structures. All the aforementioned studies did not take into account seriously the effect of carrier accumulation which is important in the type-II QW structure. It needs a calculation with the Schrödinger and the Poisson equations solved self-consistently. Liu *et al.*[8] considered the carrier accummulation and estimated the unstrained VBO to be about 0.6 eV by fitting their calculation to the experimental data for GaAsSb/GaAs QWs. However, the surface condition, which can significantly influence the band profile for the samples grown with the GaSb layer near the surface, has not yet been imposed properly on the calculations.

In this paper we demonstrate a self-consistent model that considers the surface states as a reservoir of electrons associated with pinning of the conduction band Fermi level at the midgap.[9,10] By this model, we analyze the charge distribution, the band profile, and the transition energy for GaAs/GaSb/GaAs structures under optical excitation. The resulting band profile and carrier distribution are different in character from those by the conventional symmetric band model.[2,3,8] Based on the configuration of carrier distribution, we derive a relation connecting the excitation power to the carrier density and also a relation of the transition energy shift versus the excitation power. Our model accompanied with experimental data from PL measurement is then used to determine the unstrained VBO of GaSb/GaAs. We also give a simplified version of the model that needs no self-consistent calculation. It will be useful and convenient for analyzing experimental data.

This paper is organized as follows. In Sec. II, we will describe the self-consistent model. Formulas connecting the calculation to the PL measurement will be derived in Sec. III. We will then use our theoretical model to determine the VBO of GaSb/GaAs by comparison with the measured data in Sec. IV. A simplified model and discussion with respect to it will be given in Sec. V. Finally, we draw a conclusion in Sec. VI.

[a)]Electronic mail: styen@cc.nctu.edu.tw.

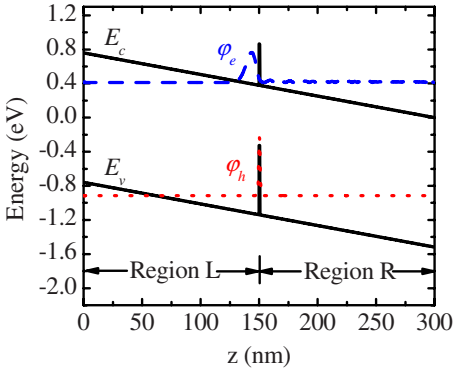

FIG. 1. (Color online) The band diagram of the GaAs/GaSb/GaAs structure grown on *n*-type substrate at thermal equilibrium. The diagram is obtained by letting the Fermi level at the surface be pinned at the midgap. The blue dashed line shows the envelope function of the conduction subband, φ_e, which is leaky in character. The red dotted line shows the envelope function of the valence subband, φ_h, which is localized in character.

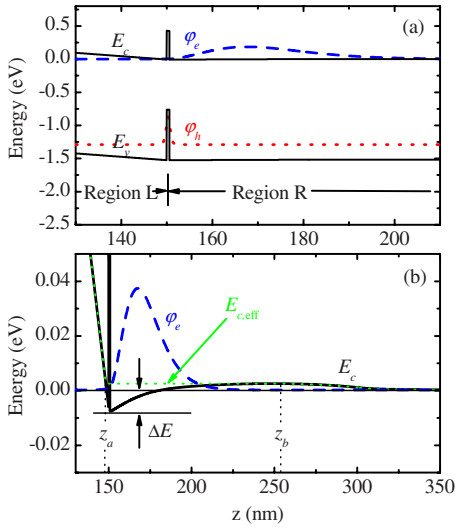

FIG. 2. (Color online) (a) The band diagram of the GaAs/GaSb/GaAs structure under sufficient optical excitation ($I > I_{\mathrm{cr}}$). There appears a localized conduction subband on the right side of the GaSb barrier, whose envelope function φ_e is shown by the blue dashed line. The band diagram and the envelope functions are obtained by the self-consistent calculation. (b) Zoom in for the conduction band profile and the envelope function around the GaSb barrier. Also shown is the profile of $E_{c,\mathrm{eff}}$, which is used for calculating the three-dimensional density of states.

II. SELF-CONSISTENT MODEL

We consider GaAs/GaSb/GaAs QW structures, as an example, which are basically the same as those in Ref. 3. They were formed with a thin GaSb layer sandwiched between two 150 nm GaAs epilayers (nominally undoped, the acceptor concentration is $N_a \approx 10^{15}$ cm^{-3}), grown on the (100) *n*-type GaAs substrate (the donor concentration is $N_d \approx 10^{18}$ cm^{-3}). In the samples there was an additional GaSb surface submonolayer ($\approx$0.5 ML) grown on the GaAs capping layer to check the thickness of the GaSb QW. In the present work, we neglect this surface layer because it will not influence significantly our calculation. Almost all the parameters in our calculation are adopted from Ref. 11. The unstrained VBO of GaSb/GaAs is set at 0.55 eV for the moment.

It is instructive first to consider the case at thermal equilibrium. In the present study, the surface states of GaAs serve as a high density-of-states reservoir of electrons such that the Fermi level can be assumed to be pinned at the midgap. At the interface between the GaAs epilayer and the GaAs substrate, the Fermi level is near the conduction band edge because of the heavily doping of the *n*-type substrate. As a result, the band profile of the GaAs/GaSb/GaAs structure can simply be drawn as shown in Fig. 1, where the GaSb QW is just inserted at the midpoint of a 300 nm GaAs layer subjected to a uniform internally built-in electric field $F_0 = E_g/2ed$ (here E_g is the band gap of GaAs, e is the elementary charge, and d=300 nm is the sum of the lengths of the GaAs epilayers). Detailed calculation considering the charge distribution in each of the layers results in an indistinguishable band profile for the samples since the charge density other than at the two end boundaries is negligibly small. The simple picture in Fig. 1 also reveals that there are excess electrons trapped by the surface states and balanced positive charge of ionized donors at the interface between the GaAs epilayer and the *n*-GaAs substrate. The excess electron density at the surface can easily be estimated to be $n_{s0} = \epsilon F_0/e = 1.85 \times 10^{11}$ cm^{-2}, where ϵ is the permittivity of GaAs.

Also shown in the figure are the envelope function φ_h of the first valence subband edge state of the GaSb/GaAs QW and the one φ_c of a quasibound conduction subband edge state confined to the left of the GaSb barrier. The valence subband states have a lifetime much longer than that of any observable electronic process so as to be regarded as localized states. On the other hand, the lifetime of the quasibound conduction subband states is as short as of the order of 10^{-12} s for a 2 ML GaSb barrier, estimated by the approach in Ref. 12. This implies that under extremely weak optical excitation, the optically generated holes can be captured and populate into the QW but the electrons cannot accumulate around the GaSb barrier. With increasing optical pumping power, more electron-hole pairs are generated and then more electrons (holes) are trapped at the surface (QW) states, leading to a higher built-in electric field F_{L} in region L which is the region of the GaAs layer to the left of the GaSb layer and screening the electric field in region R which is the region of the GaAs layer to the right of the GaSb layer.

For the pumping power I above a critical value I_{cr}, the band profile is such that there appears a localized conduction subband in region R, as illustrated in Fig. 2, and hence, electrons can accumulate around the GaSb barrier. It is obvious that for samples subjected to the critical power excitation, the band profile of region R is approximately flat and the electric field in region L is about $2F_0$ (i.e., twice the field at thermal equilibrium). Accordingly, the surface charge density at the critical condition $n_{s,\mathrm{cr}}$ is about $2n_{s0}$ ($=3.7 \times 10^{11}$ cm^{-2}). Further increasing the pumping power when $I > I_{\mathrm{cr}}$ can significantly increase the electron concentration n in region R but cause only a slight increase in the percentage of the hole concentration p in the QW because there has existed a considerable hole concentration in the QW at the critical condition $I = I_{\mathrm{cr}}$. Because of the efficient accumulation of electrons in region R, the electric field F_{L} in region L is expected to be insensitive to the pumping power above the critical condi-

tion; otherwise, a significant increase in F_L would imply an enhanced accumulation of electrons in region R, which conversely reduces F_L.

Based on the above arguments without complicated calculation, we conclude that only when $I > I_{cr}$ can significant PL involving GaSb/GaAs QW states be observed. Also we can make reasonable assumptions for our self-consistent calculation scheme appropriate to the PL experiment. In our model, the conduction and the valence band profiles are given by

$$E_c(z) = E_{c0}(z) - e\Phi(z),$$

$$E_v(z) = E_{v0}(z) - e\Phi(z), \tag{1}$$

respectively, where E_{c0} and E_{v0} are the flat band profiles of the conduction and the valence bands, respectively, and Φ is the electric potential which is the solution of the Poisson equation,

$$\frac{d}{dz}\epsilon\frac{d}{dz}\Phi = -e(p - n + N_d^+ - N_a^-). \tag{2}$$

Here, ϵ is the electric permittivity, and p, n, N_d^+, and N_a^- are the densities of holes, electrons, ionized donors, and ionized acceptors, respectively. The N_d^+ and N_a^- are given by

$$N_d^+ = \frac{N_d}{1 + 2e^{(E_{Fc}-E_d)/k_BT}},$$

$$N_a^- = \frac{N_a}{1 + 4e^{(E_a-E_{Fv})/k_BT}}, \tag{3}$$

where E_d (E_a) is the donor (acceptor) level, E_{Fc} (E_{Fv}) is the quasi-Fermi level of the conduction (valence) band, k_B is the Boltzmann constant, and T is the temperature. We set the doping concentrations at zero for the epilayers. For the hole concentration p, we consider only the holes occupying the first subband in the QW and take the parabolic band approximation, giving

$$p = |\varphi_h|^2 p_w, \tag{4}$$

where p_w is the sheet concentration of holes (in cm^{-2}) expressed by

$$p_w = \frac{k_BTm_h}{\pi\hbar^2}\ln[1 + e^{(E_h-E_{Fv})/k_BT}], \tag{5}$$

with m_h as the hole effective mass and E_h as the level of the first valence subband edge. The approximation is applicable to the case of a narrow QW under low excitation at low temperature. For the electron concentration n, we use

$$n = |\varphi_e|^2 n_w + 2\left(\frac{k_BTm_e}{2\pi\hbar^2}\right)^{3/2} F_{1/2}\left(\frac{E_{Fc} - E_{c,\mathrm{eff}}}{k_BT}\right), \tag{6}$$

where the first term accounts for the electrons occupying the first conduction subband and the second term accounts for the residual electrons that are free from the quantization confinement. n_w is the sheet concentration of electrons in the first subband expressed by

$$n_w = \frac{k_BTm_e}{\pi\hbar^2}\ln[1 + e^{(E_{Fc}-E_e)/k_BT}], \tag{7}$$

with m_e as the electron effective mass and E_e as the level of the first conduction subband edge. The omission of other subbands is because of their absence in the shallow QW, as will be the case in the present study. In the second term in Eq. (6), $F_{1/2}$ is the Fermi integral and $E_{c,\mathrm{eff}}$ is the profile of the effective conduction band edge for the three-dimensional density of states, $g_{3D}(E)\alpha\sqrt{E - E_{c,\mathrm{eff}}}$ (with E as the energy). A reasonable $E_{c,\mathrm{eff}}$ profile is set as [see Fig. 2(b)]

$$E_{c,\mathrm{eff}}(z) = \begin{cases} E_c(z_b), & z_a < z < z_b \ (z \text{ in the region of the well}) \\ E_c(z), & \text{otherwise}, \end{cases} \tag{8}$$

where z_b is the position at which $E_c(z)$ has a local maximum in region R and z_a is the position at which $E_c(z_a) = E_c(z_b)$ in region L. It is noticed that the isotropic parabolic band approximation is taken only for the simple formulas of carrier concentrations but not for calculating the envelope functions and the levels of the subband edge states. The envelope functions φ_h and φ_e associated with their energies E_h and E_e, respectively, are calculated by the eight-band $\mathbf{k}\cdot\mathbf{p}$ model.[13] The quasi-Fermi level E_{Fc} of the conduction band is assumed to be flat (and set as the energy reference) because there is no applied voltage bias and the thickness of the structure is small compared to the electron diffusion length. The Poisson equation (2) is solved under the Dirichlet boundary condition: at the surface, the E_{Fc} is assumed pinned at the midgap and at the other boundary, which is set at a place deep enough inside the substrate, the conduction band edge E_c relative to E_{Fc} is determined by the doping concentration $N_d = 10^{18}$ cm^{-3}.

A self-consistent calculation with the Schrödinger and the Poisson equations is then performed for the band profile and the carrier distributions. The charge neutrality of the whole structure is ensured by the flatness of the band inside the substrate. In the calculation, the value of the hole effective mass m_h of strained GaSb is given by Ref. 6 and all the other parameters used in the calculation are given by Ref. 11. The temperature is set at $T = 15$ K for comparision with the experiment in Ref. 3.

Now that only the holes occupying the first subband are considered, it is convenient to use the sheet density of the holes p_w as the input parameter in calculating the band profile and carrier distributions. We find that the localized conduction subband appears only when p_w is greater than a crital value p_{cr}, which is found to be 3.8×10^{11} cm^{-2}. For $p_w < p_{cr}$, the calculation based on formulas (1)–(8) cannot converge. For $p_{cr} < p_w < 4.5 \times 10^{11}$ cm^{-1}, we find that the built-in electric field in region L is almost fixed and the surface excess electron density n_s is nearly fixed at 3.75×10^{11} cm^{-2}, which is slightly higher than $2n_{s0}(=3.7 \times 10^{11}$ $cm^{-2})$ and slightly lower than p_{cr}. The increase in p_w causes only the increase in n in region R. Figure 3 shows the sheet density of the subband electrons, n_w, and the difference $p_w - n_s$ as functions of p_w. The range of p_w in

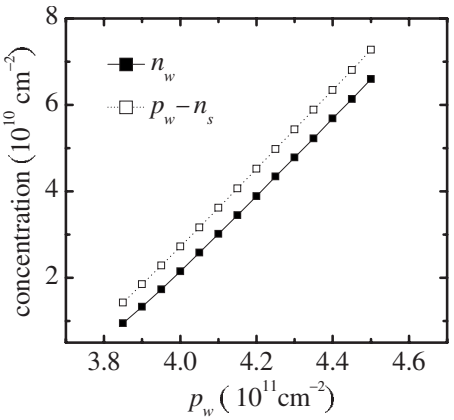

FIG. 3. The relation of $p_w - n_s$ vs p_w and that of n_w vs p_w.

the figure corresponds to the consequence that the differences, $E_{Fc} - E_e$ and $E_h - E_{Fv}$, do not exceed several meV, in accordance with our low excitation assumption. As can be seen, both n_w and $p_w - n_s$ curves are linear and parallel to each other. Accordingly, we can write

$$n_w = p_w - n_s - N_{\text{res}}, \tag{9}$$

where $N_{\text{res}} = 6 \times 10^9$ cm^{-2} is the sheet density accounting for the residual charge other than the charges of p_w, n_w, and n_s. Similar to n_s, the N_{res} is almost independent of p_w. The results and argument so far are basically independent of the thickness of the GaSb layer.

The simultaneous increase in p_w and n_w will cause deepening of the electron QW and shifting of the conduction subband edge. Figure 4 shows $\Delta E (\equiv E_e - E_{c,\min})$, which is the conduction subband edge E_e measured from the minimum of E_c (denoted by $E_{c,\min}$) as indicated in Fig. 2(b), versus $p_w - n_s$, obtained by three different calculations. The triangular potential approximation (TPA) is conventionally used to estimate ΔE. In TPA, the ΔE can be expressed by

$$\Delta E = 2.388 \left(\frac{\hbar^2 F^2}{2m_e} \right)^{1/3}, \tag{10}$$

which is obtained using an infinite triangular potential profile of a uniform electric field F to replace the realistic potential profile in region R. For

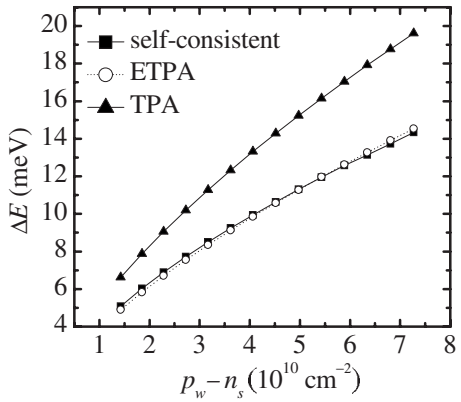

FIG. 4. The energy difference ΔE as a function of $p_w - n_s$ by three approaches: the self-consistent calculation, the ETPA, and the TPA. For ETPA, we use $\eta = 0.638$.

$$F = \frac{e}{\epsilon}(p_w - n_s), \tag{11}$$

which is the electric field at the bottom of the realistic QW, we find a significant overestimate of ΔE obtained by TPA compared to the result obtained by our self-consistent calculation, as shown in Fig. 4. The deviation is enhanced with $p_w - n_s$ increasing. It can be considerably eliminated by the effective triangular potential approximation (ETPA) that uses an average electric field

$$F = \eta \frac{e}{\epsilon}(p_w - n_s), \tag{12}$$

where η is in the range of $0 < \eta < 1$ and to be used as a fitting parameter. We find that the ΔE obtained by ETPA with $\eta = 0.638$ almost coincides with the result by the self-consisent calculation in the range of $p_w - n_s$ from 1×10^{10} to 7×10^{10} cm^{-2} The ETPA will be useful in later analysis and is also popular in device modeling.[14]

III. CONNECTION OF CALCULATION TO EXPERIMENT

To connect the theoretical calculation to the PL experiment, it is required to have a relation between the excitation power I and the hole density p_w for samples in a steady state. Under the steady state condition, the excitation of carriers is balanced by the recombination of carriers. Ledentsov *et al.*[2] gave a simple relation based on a symmetric band model in which the electron and the hole sheet densities are equal, $n_w = p_w$, in the neighborhood of the GaSb layer. As a result,

$$I = \alpha p_w n_w = \alpha p_w^2, \tag{13}$$

where the coefficient α can be obtained by fitting to experimental data.[2] With relation (13), ΔE can be expressed as a function of I by the ETPA with $F = \eta e p_w / 2\epsilon$,

$$\Delta E = 1.194 \left(\frac{\hbar^2 \eta^2 e^2}{m_e \epsilon^2 \alpha} \right)^{1/3} I^{1/3}. \tag{14}$$

This is the famous cube-root relation between the energy shift and the excitation power.[2–5] Relation (14) allows one to determine α by PL measurement of the relation of the transition energy $E_e - E_h$ versus I since ΔE is equal to the transition energy minus the separation $E_{c,\min} - E_h$, which is almost independent of I. We can then obtain the optically generated hole density p_w as a function of excitation power I by Eq. (13).

The situation is more complicated for the p_w-I and the ΔE-I relations appropriate to our model. To derive the relations, we notice that the carrier recombination process occurs primarily not only in the neighborhood of the QW but also at the surface. Since the surface states is assumed to be an electron reservoir associated with pinning of the Fermi level at the midgap, the surface recombination rate is totally determined by the flow of optically generated holes toward the surface in region L. The hole current is proportional to the product of the driving electric field F_L and the hole density. For $I > I_{\text{cr}}$ $(p_w > p_{\text{cr}})$, as has described previously, F_L is nearly independent of p_w (and thus of I). Since the hole generation rate is proportional to I, the surface recombination

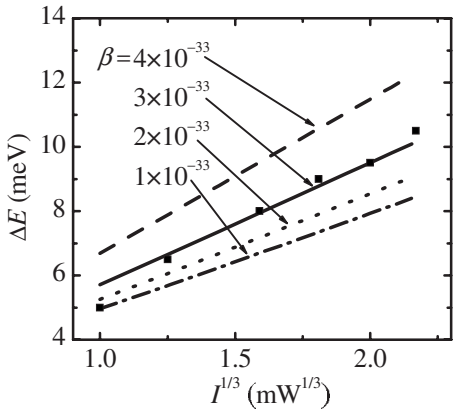

FIG. 5. The calculated energy difference ΔE as a function of the cube root of excitation power, $I^{1/3}$, with β as a parameter (in mW·cm^6). Also shown are the experimental data (denoted by the filled squares) which are obtained by shifting the data of Ref. 3 by a common energy for the structure with a 2 ML GaSb layer. They give a slope $d\Delta E/dI^{1/3} \approx 4.1$ meV/mW$^{1/3}$, corresponding to $\beta \approx 2\times 10^{-33}$ mW·cm^6.

rate should also be proportional to I. Also, since the total recombination rate is proportional to I in steady state, we conclude that the rate of radiative recombination occuring around the QW is proportional to I. Consequently, considering the optical transition from the conduction to the valence subbands, we can write

$$I \propto |\langle \varphi_h | \varphi_e \rangle|^2 p_w n_w. \tag{15}$$

The factor $|\langle \varphi_h | \varphi_e \rangle|^2$ is important in the expression because it increases with I increasing that causes deepening of the electron QW and enhances the overlap of wavefunctions. In fact, from our self-consistent calculation, we find that

$$|\langle \varphi_h | \varphi_e \rangle|^2 \propto p_w - n_s \tag{16}$$

for $p_{cr} < p_w < 5\times 10^{11}$ cm^{-2}. Using Eqs. (16) and (9) for n_w, we can rewrite Eq. (15) as

$$I = \beta (p_w - n_s)^2 p_w \left(1 - \frac{N_{res}}{p_w - n_s}\right), \tag{17}$$

where β is a coefficient that can be determined by experiment. Relation (17) with the ETPA [Eqs. (10) and (12)] allows us to calculate the energy shift ΔE versus I if β is known. Figure 5 shows the curves of ΔE versus $I^{1/3}$ obtained by our calculation with β as a parameter, and also the experimental data from Ref. 3. Strikingly, the cube-root rule for the ΔE-I relation is applied quite well to the present case. This can be understood by writing ΔE in the form

$$\Delta E = 2.388 \left(\frac{\hbar^2 \pi^2 e^2}{2 m_e \epsilon^2 n_s \beta}\right)^{1/3} I^{1/3} f, \tag{18}$$

where the factor f, defined as

$$f = \left(\frac{n_s/p_w}{1 - \frac{N_{res}}{p_w - n_s}}\right)^{1/3}, \tag{19}$$

changes slightly with the excitation power since the n_s and the N_{res} keep almost constant and the p_w changes only within a small range. For $n_s = 3.75\times 10^{11}$ cm^{-2}, $N_{res} = 6\times 10^9$ cm^{-2},

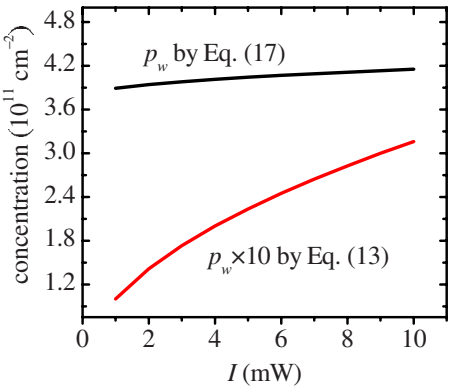

FIG. 6. (Color online) The sheet concentration of holes p_w vs the excitation power I obtained by Eqs. (13) and (17).

f varies from 1.17 to 1.03 as p_w changes from 3.9×10^{11} to 4.1×10^{11} cm^{-2}, corresponding to I changing from 1 to 10 mW, as will be seen in Fig. 6.

The PL measurement cannot give the absolute value of ΔE, as defined in Fig. 2(b), but the variation in the transition energy with I. In Fig. 5, we plot the experimental data from Ref. 3 totally by shifting a common energy. The slope of the ΔE-$I^{1/3}$ line best fit to the experimental data, which is 4.38 meV/mW$^{1/3}$, suggests the coefficient $\beta = 2\times 10^{-33}$ mW cm^6.

With the known β, we can calculate the hole concentration p_w as a function of I using Eq. (17). Figure 6 shows the p_w versus I obtained by our model using Eq. (17) as well as that by the symmetric band model using Eq. (13). As expected, p_w for our model changes slightly from 3.9×10^{11} to 4.1×10^{11} cm^{-2}, within a range of 5%, with I changing from 1 to 10 mW, while for the symmetric band model, it changes considerably in percentage. It is only the electron concentration n_w (or $p_w - n_s$) that varies significantly with I in our model.

IV. VBO DETERMINATION

To determine the VBO of GaSb/GaAs, we compare with the PL measurements[3] in Fig. 7 the calculated transition energies $E_e - E_h$ for different thicknesses d_w of the GaSb layer with the unstrained VBO as a parameter. The data in the

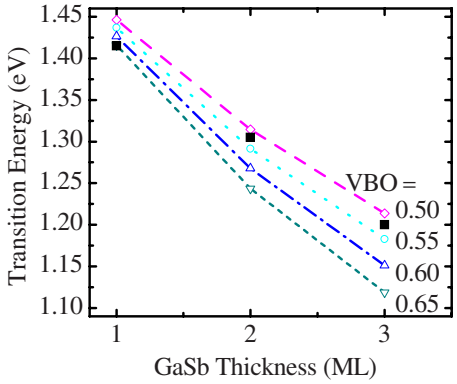

FIG. 7. (Color online) Comparison of the calculated and the measured transition energies vs the thickness of the GaSb layer. The calculated results are obtained with the unstrained VBO=0.5, 0.55, 0.6, and 0.65.

figure correspond to an excitation power of 4 mW at which the hole concentrations p_w are 4.15×10^{11} and 4.0×10^{11} cm^{-2} for $d_w=1$ and 2 ML, respectively, obtained by Eq. (17). For $d_w=3$ ML, we cannot determine the corresponding value of p_w due to insufficient experimental information for determining β. Fortunately, as has been implied by our model, the value of p_w is basically insensitive to the GaSb layer thickness for a given I. We therefore assume p_w to be 4.0×10^{11} cm^{-2} for $d_w=3$ ML. The values of p_w for the three different d_w are used as inputs in the self-consistent calculation to give the data in Fig. 7. The comparison in Fig. 7 suggests the unstrained VBO to lie between 0.5 and 0.55 eV, although the experimental and the calculated data for $d_w=1$ ML deviate from each other by about 0.03 eV (about 2%). The slight inconsistency may result from the uncertainty in the thickness of the narrow epilayer due to the difficulty in growth and/or the exchange reaction of As and Sb atoms near the interfaces.

Lo *et al.*[3] gave a similar determination of unstrained VBO but using the symmetric flat band model. Their calculated transition energy is slightly lower than ours by a factor of ΔE. As a result, Lo *et al.*[3] obtained a lower unstrained VBO of 0.4 eV.

V. DISCUSSION AND SIMPLIFIED MODEL

We have demonstrated an analysis of the electronic properties of GaSb/GaAs heterostructures under optical excitation by a self-consistent model. It is worthy to discuss the usability of our model if some constraints are released. Firstly, if the E_{Fc} at the surface is assumed not necessarily to be pinned at the midgap but at a level E_{Fcs} below the conduction band edge E_c such that there is a uniform internally built-in electric field F_0 and no localized subband in region L at thermal equilibrium, the electric field will be $F_0=(E_{Fcs}-E_{vs})/ed$ associated with an excess electron density at the surface $n_{s0}=\epsilon F_0/e$, where E_{vs} is the valence band edge at the surface. At the critical condition $I=I_{cr}$, the electric field in region L is about $F_L=(E_{Fcs}-E_{vs})/ed_L$, the surface electron density is $n_s=\epsilon F_L/e$, and the hole density in the QW is $p_w=p_{cr}$, which is slightly larger than n_s, where d_L is the thickness of region L and unnecessary to be equal to the thickness of the epilayer in region R. For $I>I_{cr}$, the F_L and hence n_s is assumed to be constant and p_w slightly increases with I. The p_w-I relation (17) is still applicable and can reasonably be written as

$$p_w = n_s + \sqrt{\frac{I}{\beta n_s}}. \tag{20}$$

In deriving Eq. (20), N_{res} in Eq. (17) is neglected and p_w is replaced by n_s for the case of low excitation and low temperature. The coefficient β can be determined by experiment using the formula

$$\beta = 6.81\frac{\hbar^2\eta^2e^2}{m_e\epsilon^2n_s}\left(\frac{d\Delta E}{dI^{1/3}}\right)^{-1/3}, \tag{21}$$

which is obtained from Eq. (18) by letting $f=1$.

The above results and argument do not depend significantly on the thickness d_w of the GaSb layer and the VBO of GaSb/GaAs if the d_w is small enough and the GaSb layer is an efficient barrier for electrons such that the ETPA is applicable. Moreover, they can also be applied to other type-II heterostructures.

The transition energy E_e-E_h is the sum of ΔE and $E_{c,\min}-E_h$. The separation $E_{c,\min}-E_h$ depends basically only on the QW width d_w and the VBO but is nearly independent of the excitation power. On the other hand, ΔE depends on the excitation power but is nearly independent of d_w and VBO. These characters allow us to determine the VBO, as in Fig. 7, without the need of a self-consistent calculation. We can use formula (18) with $f=1$ for ΔE at a given I and the eight-band method for the relation between $E_{c,\min}-E_h$ and d_w. Their sum then gives a relation between the transition energy and d_w and can be used to determine the VBO by comparison with the measured transition energy. This simplified model will be useful and convenient in analysis of the electronic and the optical properties of type-II heterostructures.

VI. CONCLUSION

We have presented a self-consistent model that can be used to analyze the charge distribution, the band profile, and the interband transition energy for GaSb/GaAs type-II QW structures under optical excitation. The model considers the surface states as an electron reservoir such that the Fermi level of the conduction band is pinned at a fixed level. In the model, the accumulation of optically generated holes in the GaSb QW causes a GaAs QW on one side of the GaSb layer which can efficiently accommodate optically generated electrons, different from the case in the conventional symmetric band model. Based on the distribution of carriers, we have derived, considering the wavefunction overlap, a relation connecting the excitation power to the generated hole density in the QW. Using the relation and the effective triangular potential approximation, we have obtained a relation between the shift of transition energy and the excitation power, which almost follows the cube-root rule. The derived formulas together with the data from PL measurement allow determining the band offset of a type-II aligned heterointerface. The result suggests the unstrained VBO to lie between 0.5 and 0.55 eV. We have also given a simplified version of the model without the need of a self-consistent calculation. It will be useful and convenient for the analysis of experimental data.

ACKNOWLEDGMENTS

This work was supported by National Science Council of the Republic of China under Contract No. 97-2221-E-009-164.

[1] M. Yano, T. Iwawaki, H. Yokose, A. Kawaguchi, Y. Iwai, and M. Inouc, Proc. SPIE **1283**, 221 (1990).
[2] N. N. Ledentsov, J. Böhrer, M. Beer, F. Heinrichsdorff, M. Grundmann, D. Bimberg, S. V. Ivanov, B. Ya. Meltser, S. V. Shaposhnikov, I. N. Yassievich, N. N. Faleev, P. S. Kop'ev, and Zh. I. Alferov, Phys. Rev. B **52**, 14508 (1995).
[3] M. C. Lo, S. J. Huang, C. P. Lee, S. D. Lin, and S. T. Yen, Appl. Phys. Lett. **90**, 243102 (2007).

[4]F. Hatami, N. N. Ledentsov, M. Grundmann, J. Böhrer, F. Heinrichsdorff, M. Beer, D. Bimberg, S. S. Ruvimov, P. Werner, U. Gösele, J. Heydenreich, U. Richter, S. V. Ivanov, B. Ya. Meltser, P. S. Kop'ev, and Zh. I. Alferov, Appl. Phys. Lett. **67**, 656 (1995).
[5]K. Matsuda, S. V. Nair, H. E. Ruda, Y. Sugimoto, T. Saiki, and K. Yamaguchi, Appl. Phys. Lett. **90**, 013101 (2007).
[6]A. Qteish and R. J. Needs, Phys. Rev. B **42**, 3044 (1990).
[7]T. Nakai and K. Yamaguchi, Jpn. J. Appl. Phys., Part 1 **44**, 3803 (2005).
[8]G. Liu, S. L. Chuang, and S. H. Park, J. Appl. Phys. **88**, 5554 (2000).
[9]J. Bardeen, Phys. Rev. **71**, 717 (1947).
[10]P. E. Gregory, W. E. Spicer, S. Ciraci, and W. A. Harrison, Appl. Phys. Lett. **25**, 511 (1974).
[11]I. Vurgaftman, J. R. Meyer, and L. R. Ram-Mohan, J. Appl. Phys. **89**, 5815 (2001).
[12]A. K. Ghatak, K. Thyagarajan, and M. R. Shenoy, IEEE J. Quantum Electron. **24**, 1524 (1988).
[13]A. Zakharova, S. T. Yen, and K. A. Chao, Phys. Rev. B **66**, 085312 (2002).
[14]T. Janik and B. Majkusiak, IEEE Trans. Electron Devices **45**, 1263 (1998).